The Plant Cell, Vol. 17, 1016–1028, March 2005, www.plantcell.org © 2005 American Society of Plant Biologists

RIN13 Is a Positive Regulator of the Plant Disease Resistance Protein RPM1 [W]

Antonious Al-Daoude,[1] Marta de Torres Zabala, Jong-Hyun Ko, and Murray Grant[2]

Department of Agricultural Science, Imperial College, London, TN25 5AH United Kingdom

The RPM1 protein confers resistance to *Pseudomonas syringae* pv *tomato* DC3000 expressing either of the Type III effector proteins AvrRpm1 or AvrB. Here, we describe the isolation and functional characterization of RPM1 Interacting Protein 13 (RIN13), a resistance protein interactor shown to positively enhance resistance function. Ectopic expression of *RIN13* (*RIN13s*) enhanced bacterial restriction mechanisms but paradoxically abolished the normally rapid hypersensitive response (HR) controlled by RPM1. In contrast with wild-type plants, leaves expressing *RIN13s* did not undergo electrolyte leakage or accumulate H_2O_2 after bacterial delivery of AvrRpm1. Overexpression of *RIN13* also altered the transcription profile observed during a normal HR. By contrast, *RIN13* knockout plants had the same ion leakage signatures and HR timing of wild-type plants in response to DC3000(*avrRpm1*) but failed to suppress bacterial growth. The modified phenotypes seen in the *RIN13s*/*as* plants were specific to recognition of AvrRpm1 or AvrB, and wild-type responses were observed after challenge with other incompatible pathogens or the virulent DC3000 isolate. Our results suggest that cell death is not necessary to confer resistance, and engineering enhanced resistance without activation of programmed cell death is a real possibility.

INTRODUCTION

Generally, plant basal defenses function successfully to prevent pathogen infection, and disease is relatively rare. When bacterial phytopathogens enter the apoplast of plants via wounds, stomata, or hydathodes, they rapidly induce a set of pathogen genes encoding a specialized structure, the Type III secretion apparatus. The type III secretion system (TTSS) acts as a conduit via which a constellation of proteinaceous products known as TTSS effectors are delivered into the host cell. The subsequent outcome of the infection is dependent upon the genetic constitution of both the host and pathogen (Espinosa et al., 2003). The successful suppression of host defenses by TTSS effectors results in disease. Alternatively, resistance pathways may be activated after the direct or indirect interaction of a specific Type III effector (the avirulence gene product) with its cognate plant disease resistance (*R*) gene product (Jin et al., 2003). Usually such gene-for-gene recognition (Flor, 1971) results in a visible hypersensitive response (HR) that effectively restricts pathogen growth.

The R proteins are key to integrating and transducing signals leading to the HR and play a central role in plant innate immune responses (reviewed in Bonas and Lahaye, 2002). Remarkably, the majority of R proteins fall into a single highly conserved class distinguished by two common structural features, the most striking being a variable number of C-terminal Leu-rich repeats (LRRs). The LRR domain is found in proteins with diverse functions and has been implicated in interactions between proteins, ligands, and carbohydrates (Jones and Jones, 1996; Kobe and Kajava, 2001). In addition, each R protein contains a conserved nucleotide binding site (NBS), which probably binds ATP or dATP (Tameling et al., 2002). The R proteins may be further subdivided depending upon the presence of either an N-terminal coiled-coil domain (CC-NBS-LRR) or *Toll*-interleukin 1 homology domain (TIR-NBS-LRR). The *Arabidopsis thaliana* genome sequence predicts ~150 NBS-LRR proteins that may confer resistance to pathogens and pests as diverse as fungi, bacteria, viruses, nematodes, and aphids (Eckardt and Innes, 2003; Meyers et al., 2003).

Hypersensitive cell death has similarities to a form of programmed cell death in mammals, known as apoptosis. Apoptotic signaling networks are activated through remarkably conserved pathways in which proapoptotic effector proteins, such as Apaf1 and Ced3, recruit and sequentially activate specific representatives of the caspase family of proteolytic enzymes (Adams and Cory, 2002). Apaf1, CED3, and other eukaryotic proapoptotic effector proteins, including those involved in response to microbial infection (Tschopp et al., 2003), contain a region of significant internal structural similarity to R proteins. This conserved domain spans the NB domain and has been variably referred to as NB-ARC (van der Biezen and Jones, 1998), the apoptopic ATPase domain (Aravind et al., 1999), or the nucleotide oligomerization domain (Inohara and Nunez, 2001, 2003). The universal prevalence of such domains suggests functional conservation in cell death effectors across plant and animal kingdoms.

[1] Current address: Atomic Energy Commission of Syria, P.O. Box 6091, Damascus, Syria.

[2] To whom correspondence should be addressed. E-mail m.grant@imperial.ac.uk; fax 44-20759-42640.

The author responsible for distribution of materials integral to the findings presented in this article in accordance with the policy described in the Instructions for Authors (www.plantcell.org) is: Murray Grant (m.grant@imperial.ac.uk).

[W] Online version contains Web-only data.

Article, publication date, and citation information can be found at www.plantcell.org/cgi/doi/10.1105/tpc.104.028720.

Many *R* genes have been isolated conferring resistance to a variety of parasites, ranging from viruses, bacteria, and fungi to aphids and nematodes (Hammond-Kosack and Parker, 2003; Martin et al., 2003). However, unlike the processes governed by the cognate mammalian proapoptotic effectors, the hierarchy of molecular interactions specified by R proteins remains unknown. In the majority of interactions, with two notable exceptions (Jia et al., 2000; Deslandes et al., 2003), no direct binding between an NB-LRR protein and its cognate avirulence (Avr) protein has been demonstrated.

Knowledge of the molecular architecture of complexes directly associated with R proteins is essential to understand the underlying mechanisms of induced defense responses. Classical forward genetic and *R* suppressor screens have identified five key loci, *EDS1*, *SGT1b*, *HSP90*, *NDR1*, and *RAR1*, required for R function (Dangl and Jones, 2001; Shirasu and Schulze-Lefert, 2003; Schulze-Lefert, 2004). NDR1, a predicted membrane spanning protein (Century et al., 1997), is differentially required by some members of the CC-NBS-LRR class of R proteins. In *ndr1-1* plants challenged with *Pseudomonas syringae* pv *tomato* DC3000 (DC3000) carrying *avrRpm1*, which recognizes the CC-NB-LRR encoding gene *RPM1* (Grant et al., 1995), a strain-specific HR is generated at ~5 h postinoculation (hpi), but plants still display enhanced susceptibility (Century et al., 1995).

RAR1, first identified in barley (*Hordeum vulgare*) (Shirasu et al., 1999) and subsequently in Arabidopsis (Muskett et al., 2002; Tornero et al., 2002b) is required for resistance by some members of both NB-LRR classes. *Atrar1* specifically attenuates HR elicited through RPM1, RPS2, and RPS5 and suppresses bacterial restriction mechanisms. A recent study suggests plant innate immune responses are modulated through association of the molecular chaperone Hsp90 with the tobacco (*Nicotiana tabacum*) viral resistance protein N and its signaling proteins SGT1 and RAR1 (Liu et al., 2004).

Furthermore, genetic studies suggest that distinct cofactors are required specifically for the function of particular NB-LRR proteins, such as RPS2 (Banerjee et al., 2001) and RPS5 (Swiderski and Innes, 2001). In the case of RPS5, the cofactor, a Ser/Thr kinase (PBS1), is proteolytically cleaved by the cognate avirulence product AvrPphB (Shao et al., 2003). The first evidence of a direct interaction of a host cofactor with an R protein was provided by the isolation of RPM1 Interacting Protein 4 (RIN4) (Mackey et al., 2002). Diminution of RIN4 suppresses both hypersensitive cell death and pathogen restriction in response to bacteria expressing *avrRpm1* and *avrB*. Surprisingly, RPS2 also physically interacts with RIN4, and AvrRpt2-dependent RIN4 disappearance is required to activate RPS2 (Axtell and Staskawicz, 2003; Mackey et al., 2003).

RIN4 was identified using the N-terminal coiled-coil domain of RPM1. To identify additional proteins that directly participate in the RPM1 signaling complex, we have used an extended version of the NB-ARC domain of RPM1 in a yeast LexA two-hybrid screen. Here, we report the isolation of a novel RPM1 interactor, RIN13, which positively modulates RPM1 resistance function. Our data support a specific and critical role for RIN13 in transducing an effective RPM1 defense response. Ectopic expression of *RIN13* confers enhanced resistance to bacteria expressing *avrRpm1* or *avrB* in the absence of hypersensitive cell death.

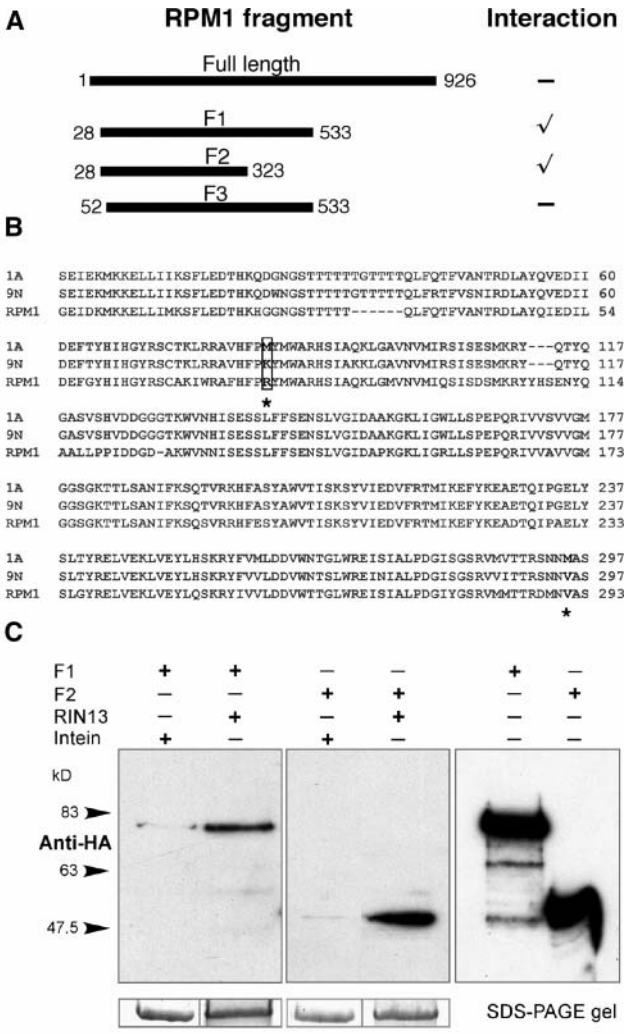

Figure 1. Characterization of the RIN13–RPM1 Interaction.

(A) Full-length RPM1, the extended RPM1 NB-ARC domain (F1), and N- and C-terminal deletions of the the NB-ARC domain (F2 and F3) were cloned into the yeast two-hybrid bait vector (pEG202), and interaction with RIN13 was tested by assaying for reporter (β-galactosidase) activity.

(B) The interaction specificity of RIN13 was tested using nearly matched endpoints of the related resistance gene *RPP5* and matched endpoint baits from *RPS2* and the *Brassica napus RPM1* alleles, *1A* and *9N*, cloned in frame into pEG202. Only 9N interacted with RIN13. In this diagram, the two most variant substitutions in 9N are indicated by an asterisk. A single nonconserved amino acid change most likely to account for the absence of an interaction between 1A and RPM1(F1), an R-to-M substitution, is boxed.

(C) RIN13 interacts with the NB-ARC domain of RPM1 in vitro. Crude bacterial extracts expressing Intein-RIN13 or an Intein control were bound to chitin beads. Crude yeast extracts expressing HA epitope-tagged F1 (left panel) or F2 RPM1 (center panel) baits (see Figure 1) were added to the beads, and the mixture was washed and binding complexes fractionated by SDS-PAGE. F1- or F2-RPM1 bound to RIN13-Intein was visualized with anti-HA antisera. The respective Intein and Intein-RIN13 Coomassie-stained loadings for each lane are shown below the immunoblot. Crude F1 and F2 fractions (1/14th of input) are shown in the right panel at right.

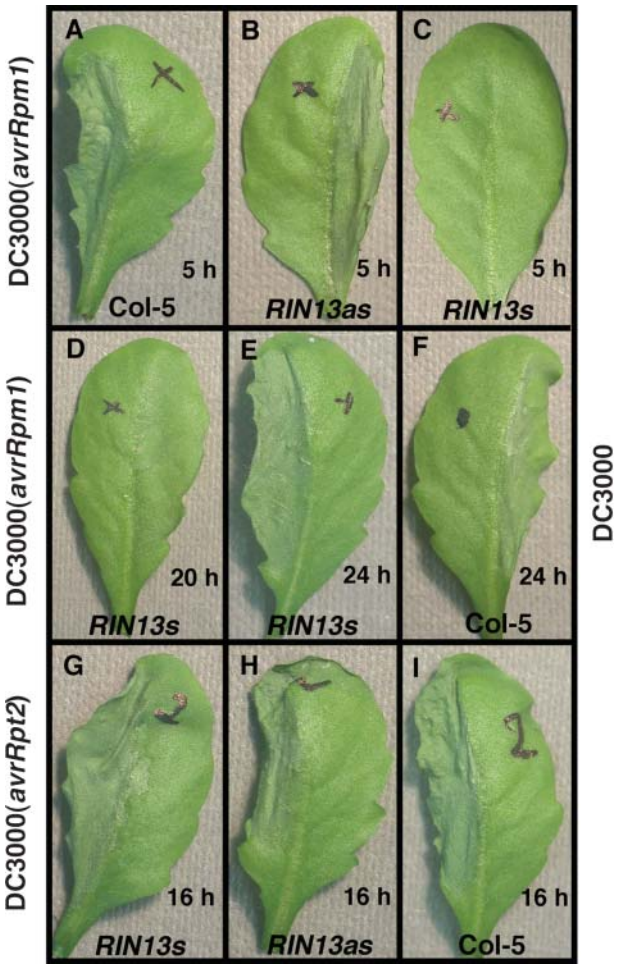

Figure 2. Overexpression of *RIN13* Suppresses the HR.

Typical interaction phenotypes for homozygous *RIN13s* and *RIN13as* lines or wild-type (Col-5) plants after challenge (inocula, 2×10^7 cfu/mL) with the following pathogens: **(A)** to **(E)**, DC3000(*avrRpm1*); **(F)**, DC3000; **(G)** to **(I)**, DC3000(*avrRpt2*). Leaves were photographed at 5 h (**[A]** to **[C]**), 16 h (**[G]** to **[I]**), 20 h **(D)**, or 24 h (**[E]** and **[F]**) after challenge. *RIN13s* lines fail to induce an HR after challenge with DC3000(*avrRpm1*), and leaves collapse coincident with those undergoing a compatible interaction (cf. **[E]** and **[F]**).

RIN13 diminution or loss of function compromised RPM1-specified restriction of bacterial growth. However, modulation of *RIN13* did not impair other gene-for-gene interactions. We conclude that RIN13 is a positive regulator of resistance and antagonizes the HR.

RESULTS

Identification and Characterization of RIN13

To identify components of the RPM1 disease resistance signaling complex, we screened an Arabidopsis LexA yeast two-hybrid cDNA prey library constructed from mRNA isolated from a mixture of uninfected Columbia-0 (Col-0) leaf tissue and tissue challenged with DC3000(*avrRpm1*) harvested at intervals up to 4 hpi as previously described (Mackey et al., 2002). As bait we used an extended region of the RPM1 NB-ARC domain (amino acids 28 to 553 of RPM1; Grant et al., 1995; Figure 1A), a module with predicted proapoptotic function highly conserved between prokaryotes and eukaryotes (Inohara and Nunez, 2003). A conditional screen for loss of RPM1 function has demonstrated a strict requirement for structural conservation within the NB-ARC domain, with >75% of *rpm1* alleles mapping within this region (Tornero et al., 2002a).

We screened 2.8×10^6 independent transformants and identified several clones exhibiting Leu auxotrophy under selective conditions that fitted the criteria of putative RINs. Applying the same convention used to describe RPM1 interactors isolated with the N terminus (~190 amino acids) of RPM1 (Holt et al., 2002; Mackey et al., 2002), our laboratory has begun naming RPM1 interactors from RIN11. Here, we describe the functional characterization of one of these interactors, RIN13.

Three independent RIN13 clones were isolated, the smallest interacting clone encoding the C-terminal 67 amino acids. We made N- and C-terminal deletions of the RPM1 bait construct to delineate the minimal interaction region. Figure 1A shows that N-terminal deletions abolished the interaction, suggesting the putative coiled-coil domain is also critical for RIN13 binding. The minimal tested portion of RPM1 sufficient for binding RIN13 comprised amino acids 28 to 323 (F2), including the P-loop and conserved Walkers A and B kinase domains of the NBS. The interaction interface excludes conserved domains 2 and 3 typical of *R* gene products (Grant et al., 1995).

Next, we examined the specificity of the interaction by constructing nearly matched endpoint baits from *RPP5* (van der Biezen et al., 2000) and matched endpoint baits from *RPS2* and the *Brassica napus RPM1* alleles, *1A* and *9N* (Grant et al., 1998). All bait constructs were verified for nuclear localization in yeast as defined by LacZ repression assays and lack of transcriptional activation. RIN13 only interacted with the cognate domain encoded by the *B. napus RPM1 9N* allele. A single nonconserved amino acid substitution distinguishes 1A from the paralogous 9N NB-ARC domain, therefore defining a critical residue for RIN13 binding in yeast (Figure 1B). No interaction was detected with AvrRpm1, AvrB, or RIN4.

Table 1. Summary of the Timing of Macroscopic Leaf Collapse in Wild-Type (Col-5) and Transgenic Lines

	Initial Time of Macroscopic Leaf Collapse (h)		
Pathogen	Col-5	*RIN13s*	*RIN13as*
DC3000	24	24	24
DC3000 (*avrRpm1*)	5	24	5
DC3000 (*avrB*)	5	24	5
DC3000 (*avrRpt2*)	16	16	16

Leaves were challenged with high inocula (2×10^7 cfu/mL) of near-isogenic pathogens that differed only by the presence or absence of a particular avirulence gene. Timing (hpi) reports when all challenged leaves showed visible collapse.

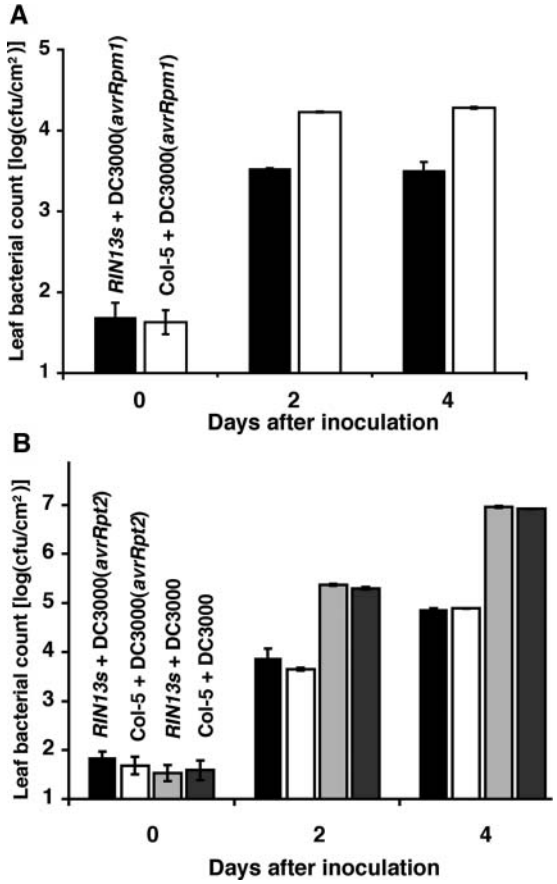

Figure 3. RPM1-Mediated Resistance Is Enhanced by Ectopic Expression of *RIN13*.

(A) Overexpression of *RIN13* enhances resistance specified by RPM1. Bacterial growth was compared in *RIN13s* (black bars) with Col-5 (white bars) after challenge with DC3000(*avrRpm1*) resuspended to 0.8×10^5 cfu/mL. Each growth measurement represents the average bacterial count derived from six plants, sampling three leaves/plant at each time point. The results were repeated three times with similar results.

(B) *RIN13* overexpression does not affect resistance responses elicited by unrelated *R* genes or the virulent carrier isolate. Leaf discs were sampled at the appropriate time after the following challenges: *RIN13s* with DC3000(*avrRpt2*) (black bars) or DC3000 (light-gray bars) and Col-5 with DC3000(*avrRpt2*) (white bars) or DC3000 (dark-gray bars). The experiment was repeated three times, and in all cases no difference in bacterial growth could be distinguished between the treatments.

An Arabidopsis cDNA library was screened with the largest prey insert (~550 bp). A full-length *RIN13* cDNA containing a 197-nucleotide 5′ and a 176-nucleotide 3′ untranslated region was isolated and sequence verified against the Arabidopsis genomic database (www.arabidopsis.org). The 1293-nucleotide open reading frame encodes a 430–amino acid protein of ~47,900 molecular weight with no discernible peptide domain or motif homology at the primary sequence level (see Supplemental Figure 1 online). RIN13, designated At2g20310.1, is a member of a two-gene family in Arabidopsis sharing 32% identity and 42% similarity to At4g28690.1. In silico searches predict that RIN13 is unique to plants with orthologs present in the rice (*Oryza sativa*) database.

RIN13 transcript could not be detected on RNA gel blots derived from unchallenged leaves or leaf tissue previously challenged with either a compatible or incompatible pathogen (data not shown). The low level of *RIN13* transcript is in agreement with the limited occurrence in the Arabidopsis EST database and the negligible or absent hybridization of the *RIN13* probe set (265307_at) during a variety of pathogen-challenged and control GeneChip (At-1) experiments (http://affymetrix.arabidopsis.info/narrays/experimentpage.pl?experimentid=59). Moreover, full-length *RIN13* self-activated in the yeast two-hybrid system, precluding screening for interactions with full-length RPM1, AvrRpm1, AvrB, or RIN4.

RIN13 Interacts with the NB-ARC Domain of RPM1 in Vitro

Full-length RIN13 either with or without a hexahistidine epitope tag could not be expressed in a prokaryotic expression system. RIN13 could only be successfully expressed as a chimeric fusion to an N-terminal domain, such as maltose binding protein or intein. Peptide antibodies raised to N- and C-terminal domains of RIN13 recognized chimeric RIN13 protein. Intein-RIN13 was used for in vitro pull-down experiments with crude yeast extracts expressing either RPM1 F1 or F2 containing an N-terminal influenza virus hemagglutinin (HA) epitope tag. Figure 1C shows that Intein-RIN13 containing a chitin binding domain, but not intein alone containing a chitin binding domain, can efficiently pull down F1-HA or F2-HA from crude yeast extracts, providing strong evidence that full-length RIN13 can bind to the NB-ARC domain of RPM1.

Overexpression of *RIN13* Abolishes Hypersensitive Cell Death

To investigate the role of *RIN13* in *RPM1*-mediated resistance, we first generated independent transgenic lines of Arabidopsis Col-5 expressing an antisense fragment of *RIN13* (*RIN13as*) under control of the strong viral 35S promoter or the full-length *RIN13* open reading frame driven off the 35S promoter (*RIN13s* lines). For each construct, 24 independent T1 lines were selected. *RIN13s* transcripts were visualized after RNA gel blot analysis. Expression levels in *RIN13s* were significantly lower than normally attained in our laboratory from genes driven off the 35S promoter of *Cauliflower mosaic virus* (data not shown), suggesting possible selection for transgenes with lower expression levels. However, all T1 lines tested were phenotypically normal and showed no developmental or morphological defects.

We compared the response of 24 antisense and 24 overexpression transgenic lines to different DC3000 isolates by leaf phenotype assays using a bacterial concentration of 2×10^7 colony-forming units (cfu)/mL. All challenged *RIN13as* leaves exhibited the characteristic RPM1 HR with macroscopic leaf collapse occurring ~5 hpi with DC3000(*avrRpm1*) (Figures 2A and 2B). Leaves challenged with the virulent DC3000 strain collapsed ~24 h after challenge, mirroring the wild-type response to DC3000. Fascinatingly, and in contrast with the *RIN13as* leaf phenotype, 17/24 *RIN13s* T1 plants challenged

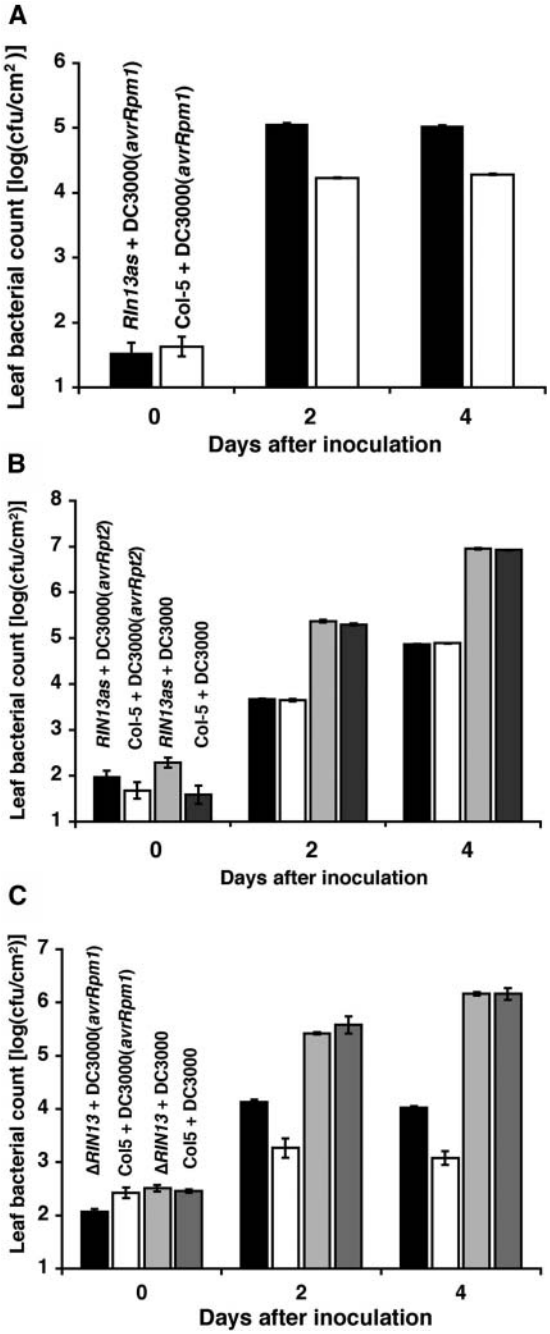

Figure 4. Reduction in *RIN13* Expression Results in Enhanced Susceptibility to DC3000(*avrRpm1*) but Not DC3000 or DC3000 Carrying *avrRpt2*.

(A) Bacterial growth was significantly enhanced in *RIN13as* (black bars) lines compared with Col-5 (white bars) after challenge with DC3000 (*avrRpm1*). The results were repeated at least three times with similar results.

(B) *RIN13* diminution does not modify responses to bacteria carrying *avrRpt2*. Bacterial growth in *RIN13s* leaves [DC3000(*avrRpt2*) (black bars) or DC3000 (light-gray bars)] was identical to growth measured in Col-5 control leaves inoculated with DC3000(*avrRpt2*) (white bars) or DC3000 (dark-gray bars). The experiment is representative of three replicates.

with DC3000(*avrRpm1*) did not undergo macroscopic leaf collapse at 5 h (Figure 2C), and leaf collapse was not evident even at 20 hpi (Figure 2D). Challenged leaves of *RIN13s* plants collapsed at ~24 hpi (Figure 2E), almost identical timing of collapse as observed after challenge with the virulent DC3000 isolate on Col-5 leaves (Figure 2F). Moreover, all challenged *RIN13s* leaves on independent plants responded in a consistent and synchronous manner.

To determine whether recognition specificities to other *R* gene combinations were affected, we tested the ability of *RIN13s/as* lines to trigger the HR against isogenic strains of DC3000 (*avrRpt2*). *RIN13s* (Figure 2G) and *RIN13as* (Figure 2H) leaves collapses at ~16 hpi after challenge with DC3000(*avrRpt2*), consistent with the wild-type RPS2-mediated HR (Figure 2I). These leaf phenotype results are summarized in Table 1. Similarly, macroscopic responses of the transgenic lines to bacterial challenges with *avrRps4* or *avrPphB*, which respectively recognize the TIR-NBS-LRR RPS4 and CC-NBS-LRR RPS5 resistance proteins, were wild-type (data not shown). We also examined the response of *RIN13s/as* to infection with the obligate parasite *Peronospora parasitica*. No difference in sporulation or degree of resistance was observed between *RIN13* transgenics and wild-type controls after inoculation with the virulent Emco5 or avirulent Cala2 isolates (Holub et al., 1995).

RIN13s Plants Have Enhanced Resistance to Bacteria Carrying *avrRpm1*

Hypersensitive cell death is traditionally associated with pathogen restriction. We investigated the ability of *RIN13s* lines to suppress bacterial growth after challenge with DC3000 or DC3000 carrying either *avrRpm1* or *avrRpt2*. For each construct, two homozygous lines with the highest transgene expression were selected to determine effects on bacterial growth. Figure 3A shows that *RIN13s* plants challenged with DC3000(*avrRpm1*) significantly reduced bacterial growth compared with the wild-type *avrRpm1/RPM1*-mediated resistance. Identical results were obtained in triplicate experiments using two independent T2 lines homozygous for the transgene. Similar hyperrestriction of bacterial growth in the absence of the HR were obtained after challenge with DC3000(*avrB*) (data not shown).

By contrast, bacterial growth in *RIN13s* transgenic lines was as in wild-type leaves after challenge with DC3000(*avrRpt2*) or the virulent DC3000 parental strain (Figure 3B). Overexpression of *RIN13* therefore abolishes hypersensitive cell death but paradoxically, also enhances bacterial restriction in leaves undergoing RPM1 defense responses. We conclude that RIN13 positively enhances RPM1 bacterial restriction mechanisms, and excess

(C) *RIN13* knockout plants phenocopy the enhanced susceptibility of *RIN13as* lines. Levels of bacterial growth were significantly enhanced in leaves of Δ*RIN13* compared with Col-5 plants after challenge with DC3000(*avrRpm1*) (black and white bars, respectively). As expected, no differences were measured in response to challenge with virulent DC3000 (light-gray and dark-gray bars, respectively). These assays were repeated twice with similar results.

RIN13 suppresses the ability to engage signaling pathways leading to hypersensitive cell death.

RIN13as Lines Display Enhanced Susceptibility to Bacteria Expressing *avrRpm1*

In contrast with *RIN13s* lines, *RIN13as* plants showed a significant increase in bacterial growth after challenge with DC3000 (*avrRpm1*) (Figure 4A). This effect was specific to the *RPM1*/*avrRpm1* interaction. Pathogen responses were otherwise wild-type after inoculation with either DC3000 or DC3000(*avrRpt2*) (Figure 4B) or infection with the avirulent *P. parasitica* isolate Cala2 (data not shown). These data are consistent with a specific role for RIN13 in activating RPM1 signaling pathways leading to restriction of bacterial growth.

Because *RIN13* transcripts are not detectable by conventional RNA gel blots, we could not accurately quantify the level of suppression of *RIN13* in *RIN13as* plants. We therefore identified a homozygous *RIN13* knockout (Δ*RIN13*; SALK_001145; see Supplemental Figure 1 online) containing a T-DNA insertion at position 345 of the predicted open reading frame (Alonso et al., 2003). Unchallenged Δ*RIN13* plants showed no obvious visible phenotype. As predicted from *RIN13as* lines, the timing of leaf collapse was identical in Δ*RIN13* lines and parental Col-0 (*RPM1*) plants challenged with DC3000(*avrRpm1*) or in Δ*RIN13* crossed into the Col-5 background. Similarly, bacterial growth measurements showed Δ*RIN13* lines supported increased multiplication compared with Col-5 when challenged with bacteria carrying *avrRpm1* (Figure 4C), suggesting RIN13 is specifically required for full AvrRpm1-specified resistance. No differences from wild-type bacterial growth levels were observed after challenge with DC3000 (Figure 4C) or DC3000 carrying *avrRpt2* (data not shown). We conclude that RIN13 is not required for signaling the HR and that when overexpressed acts to suppress hypersensitive cell death.

RIN13 Is Dependent upon RPM1 Function

After the demonstration of in vitro interaction between RIN13 and RPM1 (Figure 1C), extensive efforts were made to demonstrate an in vivo interaction using both ectopically expressed native and epitope-tagged *RIN13* constructs in *RPM1-myc* transgenic lines (Boyes et al., 1998). No expression of the epitope-tagged protein could be detected in any line. Furthermore, C-terminal epitope tags appeared to abolish the *RIN13* overexpression phenotype. These data indicate a strong selection against high levels of RIN13, despite no developmental or pleiotrophic effects in ectopic or knockout *RIN13* plants. Moreover, markers indicative of activated defense responses, such as *PR1*, were not induced (data not shown).

We next examined interaction phenotypes and bacterial growth in *RIN13s* and *RIN13as* lines generated in *rpm1*-3 (Grant et al., 1995) or *Atrar1*-28 (Tornero et al., 2002b) genetic backgrounds. All lines underwent a normal defense response conditioned by their specific genetic background: enhanced bacterial growth of DC3000(*avrRpm1*) and no HR (see Supplemental Figure 2 online; Table 2). Results from visible phenotypes and bacterial growth assays derived from Figures 2 to 4 are summarized in Table 2. We conclude that (1) RIN13 function depends upon *AtRAR1*, and (2) hyperresistance and cell death suppression in *RIN13s* lines requires delivery of AvrB or AvrRpm1 and the presence of functional RPM1 protein.

Table 2. Summary of the Effects of Ectopic and Antisense *RIN13* Expression in Col-5 Wild-Type and Mutant Backgrounds

	Plant Line Tested with DC3000(*avrRpm1*)				
Parameter	Col-5	*RIN13s*	*Rin13as*	*Atrar1*-28 (*RIN13/as*)	*rpm1*-3 (*RIN13s/as*)
Bacterial growth	++	+	++++	++++	+++++
HR	+++	–	+++	–	–

The table summarizes restriction of bacterial growth and strength of the visible HR after challenge with DC3000 carrying *avrRpm1*. Data are summarized from Figures 2 to 5. The strength of the response measured ranges from absent (–) to the strongest observed (+++++).

RIN13 Expression Modifies Physiological Responses

Changes in ion fluxes are one of the first measurable events during the initial establishment of the HR and provide a robust method for tracking and quantification of cellular collapse (Bestwick et al., 1998). Conductivity measurements from water containing leaf discs of *RIN13s*, Δ*RIN13*, or Col-5 leaves challenged with DC3000(*avrRpm1*) showed that electrolyte leakage from Δ*RIN13* or Col-5 leaf discs was indistinguishable, consistent with an accumulation of ions in the media because of irreversible membrane damage (Figure 5A). By contrast, electrolyte leakage from *RIN13s* leaf discs inoculated with DC3000(*avrRpm1*) showed only ~10% of ion leakage associated with a wild-type incompatible response and was virtually indistinguishable from that observed in a wild-type compatible interaction. Because electrolyte leakage is a measure of membrane integrity, these data provide compelling evidence that RIN13 overexpression suppresses RPM1-mediated cell death.

In *RIN13s* leaves challenged with DC3000(*avrRpm1*), collapse occurred at the same time as in wild-type leaves inoculated with the virulent DC3000 isolate (Figures 2E and 2F). *RIN13s* leaves challenged with DC3000(*avrRpm1*) showed little uptake of the vital dye, trypan blue (Koch and Slusarenko, 1990), even at 17 hpi (Figure 5B, panels A, D, and E) consistent with absence of cell death. In contrast with *RIN13s* leaf cells (Figure 5B, panel A), *RIN13as* (Figure 5B, panel B) and Col-5 leaves (Figure 5B, panel C) showed confluent trypan blue staining 6 hpi, consistent with membrane damage associated with a HR. Similar confluent trypan blue staining was not evident in *RIN13s* leaves until 24 hpi (Figure 5B, panel F).

Increases in reactive oxygen intermediates (ROIs), predominately the superoxide anion O_2^- and hydrogen peroxide (H_2O_2), are often associated with elaboration of an HR, including the response observed in the incompatible *avrRpm1*/*RPM1* interaction (Grant and Loake, 2000; Grant et al., 2000). In the absence of trypan blue staining, we examined ROI generation after DC3000(*avrRpm1*) challenge by visualizing H_2O_2 accumulation

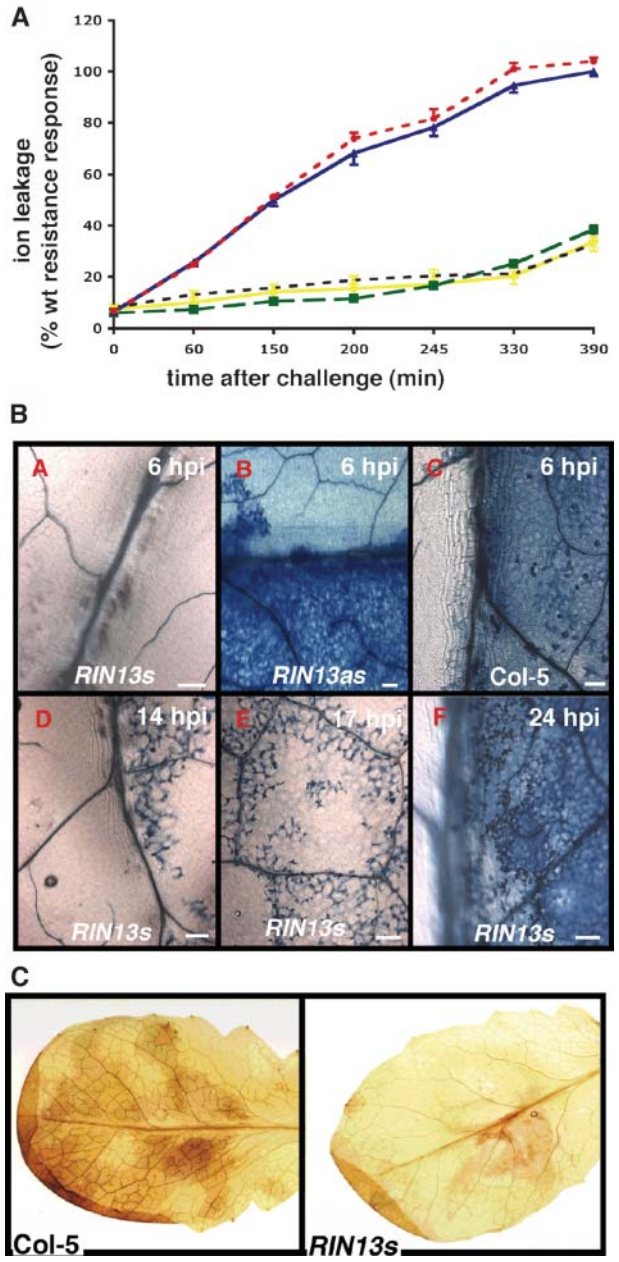

Figure 5. Changes in *RIN13* Expression Modify Physiological Responses after RPM1 Elicitation.

(A) Electrolyte leakage is suppressed in *RIN13s* but not in Δ*RIN13* lines after RPM1 elicitation. Ion leakage in Δ*RIN13* leaves challenged with DC3000(*avrRpm1*) (red) was indistinguishable from a wild-type (Col-0) resistance response (blue). However, similarly challenged *RIN13s* lines (black) exhibited restricted ion leakage identical to DC3000-challenged Col-0 (yellow) or *RIN13s* (green) leaves.

(B) Cell death is suppressed in *RIN13s* but not Δ*RIN13* leaves in response to an avirulent pathogen. Lactophenol trypan blue exclusion staining was used to monitor cell viability after challenge with DC3000(*avrRpm1*). At 6 hpi, no cell death was evident in *RIN13s* leaves (panel A) in contrast with Δ*RIN13* (panel B) and control leaves (panel C). Isolated microscopic patches of dying cells were detected at 14 hpi (panel D) and with increasing frequency (17 hpi, panel E) until confluent staining at 24 hpi (panel F).

(C) *RIN13s* leaves fail to accumulate H_2O_2 during an incompatible response. H_2O_2 accumulation was measured by DAB polymerization (Thordal-Christensen et al., 1997) in leaves harvested 4 hpi with DC3000(*avrRpm1*). Macroscopic reddish-brown deposits characteristic of ROI generation were detected in the wild type but not in *RIN13s* leaves, indicative of suppression of ROI generation mechanisms.

using 3,3-diaminobenzidine (DAB) polymerization (Thordal-Christensen et al., 1997). Reddish brown solvent stable DAB deposits were detected 5 hpi in *RIN13as* (data not shown) and Col-5 leaves (Figure 5C) but, strikingly, not in *RIN13s* leaves after DC3000(*avrRpm1*) challenge (Figure 5C). These data imply that *RIN13* overexpression attenuates ROI generation after challenge with DC3000(*avrRpm1*), and early increases in ROIs are not required for suppression of bacterial growth.

Suppression of Hypersensitive Cell Death Is Not the Result of Interference with Bacterial Delivery of AvrRpm1

We have recently demonstrated that biophoton generation is a robust, nondestructive marker of gene-for-gene specified hypersensitive cell death (Bennett et al., 2005). After DC3000 (*avrRpm1*) challenge, biophoton emission was not detected in *RIN13s* leaves, although typically strong bioluminescence was distinguishable in control Col-5 plants beginning ~2.5 hpi (Figure 6B). These data reinforce that even though DC3000 (*avrRpm1*)-challenged *RIN13s* cells die after 24 h, they do not show a typical RPM1 biophoton signature, consistent with abrogation of the HR. In support of this observation, *RIN13s* leaves challenged with either DC3000 or DC3000(*avrRpm1*) exhibit weak biophoton emission ~18 to 22 hpi, characteristic of DC3000-inoculated Col-5 plants (Bennett et al., 2005; see Supplemental Figure 3 online). However, identical biophoton signatures were measured in Col-5 and *RIN13s* plants after challenge with DC3000 expressing either *avrRpt2* or *avrRps4* (data not shown), reinforcing the observation that RIN13 functions specifically in RPM1 resistance.

To preclude that overexpression of *RIN13* interferes with AvrRpm1 delivery, we examined biophoton generation in an F1 cross between *RIN13s* plants and Col-5 plants conditionally expressing *avrRpm1* under control of the dexamethasone glucocorticoid receptor (Dex:*avrRpm1*). After DEX application (10 μM) or DC3000(*avrRpm1*) challenge, wild-type Dex:*avrRpm1* plants emitted biophotons at ~2.5 hpi (Figure 6D). By contrast, neither DEX application nor DC3000(*avrRpm1*) challenge generated biophotons in *RIN13s*/Dex:*avrRpm1* leaves (Figure 6D) nor resulted in a subsequent HR. These data indicate RIN13 acts to abolish the in planta HR inducing activity of AvrRpm1, as opposed to the RIN13-enhanced resistance resulting in abrogation of AvrRpm1 delivery through the TTSS.

RIN13s Lines Exhibit Modified Expression Profiles

We extended our phenotypic and physiological data to examine how *RIN13s* lines modified normal RPM1 signal transduction

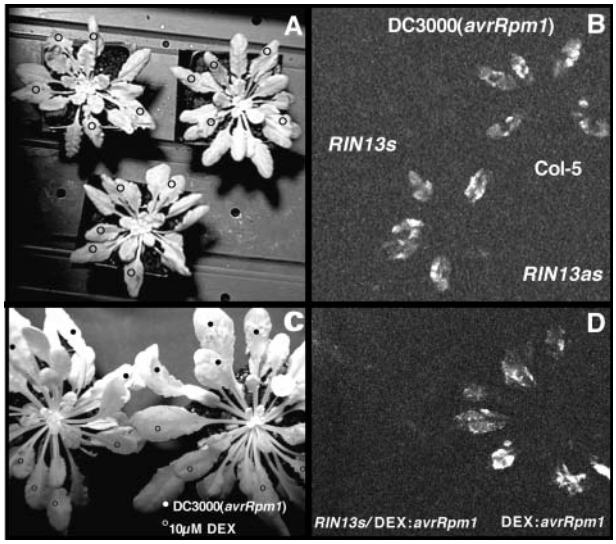

Figure 6. Biophoton Generation Is Abolished in *RIN13s* Lines after Challenge with DC3000(*avrRpm1*) or Conditional Expression of *avrRpm1*.

(A) Bright-field image of *RIN13s*, *RIN13as*, and control Col-5 plants challenged with DC3000(*avrRpm1*) (open circles).
(B) No biophoton emission was detected in inoculated *RIN13s* leaves, consistent with the absence of the HR (Bennett et al., 2005).
(C) Bright-field image of *RIN13s*/DEX:*avrRpm1* and DEX:*avrRpm1* lines immediately after application of 10 μM DEX (open circles) or inoculation with DC3000(*avrRpm1*) (A_{600} 0.05).
(D) Strong biophoton emission is detected in DEX:*avrRpm1* plants after either bacterial inoculation or DEX application but not in the *RIN13s*/DEX:*avrRpm1* line.

pathways. Total RNA was isolated from Col-5 or *RIN13s* plants at 0, 2, or 4 hpi with DC3000(*avrRpm1*). RNA gel blots were probed with two markers specific to *RPM1*-mediated resistance, *RIPK* (*RPM1 induced protein kinase*) and *TONB*, encoding a predicted chloroplast localized protein (de Torres et al., 2003). Figure 7 shows enhanced induction of the *RIPK* in *RIN13s* plants compared with Col-5 after DC3000(*avrRpm1*) challenge. By contrast, *TONB* message is markedly reduced in *RIN13s* plants relative to transcript levels in Col-5. Thus, *RIN13s* lines show modification of early transcriptional reprogramming events specified by RPM1. The enhanced induction of *RIPK* suggests a role for this kinase in modulating the bacterial restriction component of RPM1 function.

DISCUSSION

RIN13 Is a Positive Regulator of RPM1-Specified Resistance

The product of the resistance gene *RPM1*, like other R proteins, is predicted to function as part of a signaling complex localized to the peripheral plasma membrane and comprising associated host proteins that serve either as targets of AvrB and AvrRpm1 or as linker proteins to mediate Avr/R recognition (Grant and Mansfield, 1999). Previous two-hybrid screens have identified RIN2 and RIN4 binding to the N-terminal 190 amino acids of RPM1. Here, we report the isolation and characterization of another component of this complex, RIN13. Modulation of *RIN13* expression differentially impacts two fundamental attributes of resistance responses, hypersensitive cell death, and restriction of pathogen growth. *RIN13* overexpression abolishes the rapid HR (~5 h) normally elicited by RPM1 but, paradoxically, positively regulates RPM1 function, resulting in significant enhancement of bacterial restriction. By contrast, RIN13 knockout plants undergo wild-type HR, but their ability to restrict growth of bacteria carrying *avrRpm1* is significantly compromised.

The specificity for RPM1 function and the absence of morphological and developmental defects in *RIN13s* lines contrasts with other mutations that lead to resistance without the HR. For example, the Arabidopsis mutants *dnd1* (Clough et al., 2000) or *hlm1* (Balague et al., 2003), encoding the cyclic nucleotide-gated ion channels CNGC2 and CNGC4, respectively, fail to generate an HR in response to several *P. syringae* pathogens but still conduct effective pathogen restriction. However, unlike *RIN13*, both mutants are strongly dwarfed, have elevated mRNAs for pathogenesis-related genes, and under certain conditions develop spontaneous lesions. The *dnd1*-type mutant probably has constitutively elevated basal defense that restricts bacterial multiplication without the HR. The altered ion homeostasis in such mutants may activate basal resistance by effectively imposing an abiotic stress and underline the importance of ion homeostasis in signaling pathways leading to HR and resistance (Balague et al., 2003).

We demonstrated that leaves of *RIN13s* plants challenged with DC3000(*avrRpm1*) exhibited leaf collapse coincident with those challenged by the virulent DC3000 isolate. The absence of rapid H_2O_2 accumulation and trypan blue staining and the late biophoton generation (see Supplemental Figure 3 online) suggest that this *RIN13s* leaf collapse is similar to that induced by DC3000. As with all bacterial leaf-spotting pathogens, susceptible accessions of DC3000 only remain biotrophic for 1 or 2 d before the host tissue eventually dies at the inoculation site. The associated tissue collapse during the compatible interaction was described as normosensitive collapse by Klement (1982) to distinguish it from the more rapid HR observed in resistant

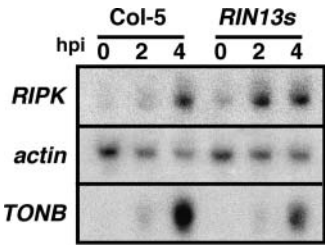

Figure 7. RPM1-Elicited *RIN13s* Plants Have Modified Gene Expression Patterns.

The induction of *RPM1*-specific gene transcripts (de Torres et al., 2003) was monitored after DC3000(*avrRpm1*) challenge (2×10^7 cfu/mL). *RIN13s* plants showed enhanced induction of *RIPK* compared with wild-type plants. By contrast, induction of the *TONB* transcript was significantly delayed in *RIN13s* lines.

plants. Even using high inoculum concentrations, cell death in response to wild-type DC3000 is not preceded by a strong oxidative burst or increases in cytosolic calcium, thus differentiating it from the HR occurring as a result of the avrRpm1/RPM1 interaction described here. Death of plant cells during tissue colonization by DC3000 may be a direct result of the cumulative activity of effector proteins on cytoplasmic targets, such as the cytoskeleton and signal transduction pathways, as observed in bacterial pathogenesis of animal cells (Buttner and Bonas, 2003). Although normosensitive collapse does not appear to be programmed cell death as observed during the HR, the proposal that the HR is an accelerated development of a compatible interaction (Klement, 1982) has gained support from recent transcriptional profiling studies (Tao et al., 2003).

RIN13s Plants Exhibit Modified Physiological and Molecular Infection Signatures

In *RIN13s* plants, enhanced resistance is associated with minimal electrolyte leakage (Figure 5A), limited microscopic cell death (Figure 5B), no obvious RPM1-dependent oxidative burst, as indicated by greatly reduced staining of the inoculated zone with DAB (Figure 5C), and absence of biophoton emission (Figure 6). Although the HR is generally thought to be intimately associated with resistance, our data suggest that signaling through R protein complexes, even in strong *R* genes such as *RPM1* (Mackey et al., 2002), can be modulated to enhance bacteria restriction yet abrogate cell death.

Interestingly, H_2O_2 accumulation in *RIN13s* plants is minimal and apparently not a requisite for the cellular processes required to restrict bacterial growth. These observations are supported by studies in the Arabidopsis respiratory burst oxidase homolog D mutant (*AtrbohD*). DC3000(*avrRpm1*)-challenged *AtrbohD* leaves did not accumulate H_2O_2 accumulation, but the HR and bacterial restriction were wild-type (Torres et al., 2002).

Ectopic expression of *RIN13* also modified the molecular signature associated with the archetypical RPM1 resistance. Induction of *RIPK* transcript is accelerated in *RIN13s* lines. Conversely, in *Atrar1* and *rpm1* mutants, *RIPK* expression is suppressed after RPM1 elicitation (de Torres et al., 2003), correlating *RIPK* induction with bacterial restriction. By contrast, *TONB* expression is delayed in both *Atrar1* and *RIN13s* lines, both of which exhibit significant or total suppression of the classical RPM1 HR. Therefore, *TONB* expression positively correlates with the HR. These data suggest that global expression profiling of *RIN13s/as* lines will reveal comparative molecular signatures specifying the (1) enhanced resistance and reduced cell death and (2) enhanced susceptibility and normal HR phenotypes generated by *RIN13* misexpression after RPM1 elicitation. Data emerging from such studies will make a valuable contribution to understanding how these two response pathways are elaborated after pathogen recognition.

What Are the Possible Mechanisms of RIN13 Action?

The guard hypothesis (Van der Biezen and Jones, 1998; Dangl and Jones, 2001) predicts that in the absence of the matching R protein, the primary role of many Avr proteins (like other bacterial Type III effectors) is to target unknown determinants of susceptibility within the host. Emerging evidence also suggests that the R protein conformation plays an important role in regulatory control. Initial models predict specificity resides in the LRR domain of R proteins (Moffett et al., 2002); however, genetic studies of flax *F* alleles suggest that amino acids outside the LRR domain also contribute to recognition specificity (Luck et al., 2000). For example, intramolecular interactions at the N terminus regulate function of the CC-NBS-LRR potato (*Solanum tuberosum*) viral resistance protein Rx. Although functional Rx could be generated in trans through expression of modular domains (Moffett et al., 2002), direct or indirect elicitor perception disrupts this interaction. These data suggest that conformational changes after elicitation are necessary for signaling through R proteins. RIN4 represents the archetypical guardee to support both above models (Axtell and Staskawicz, 2003; Mackey et al., 2003). Conformational restrictions appear to constrain RIN4 binding to RPM1 in yeast two-hybrid studies (Mackey et al., 2002). RIN4

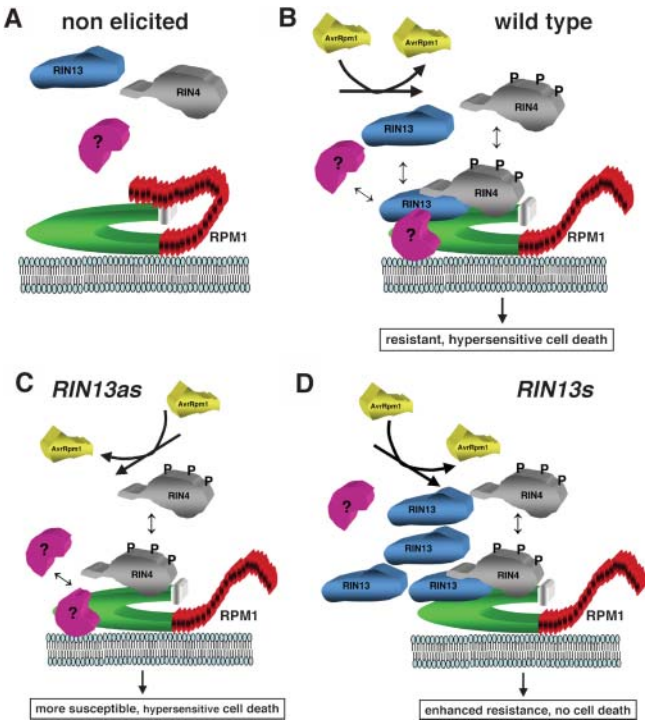

Figure 8. Model for RIN13 Function.

In the nonelicited state, RPM1 adopts a conformational state in which the RIN13 binding site in the NB-ARC domain is buried **(A)**. Upon elicitation, conformational changes, possible induced by AvrRpm1 phosphorylation of RIN4, expose the RIN13 binding site and allow RIN13 to cooperate in normal defense signaling processes in conjunction with one or more unknown interactors (?) **(B)**. In Δ*RIN13* lines, absence of RIN13 prevents elaboration of full wild-type resistance responses but does not compromise signaling through pathways that elicit hypersensitive cell death **(C)**. By contrast, overexpressed RIN13 preferentially occupies binding sites that activate bacterial restriction mechanisms. Simultaneously, RIN13 occupation prevents or hinders signaling components that activate the HR resulting in suppression of cell death **(D)**.

interacted strongly with the N-terminal 176 amino acids of RPM1 but very weakly with amino acids 55 to 341 of RPM1, implying that either the coiled-coil containing amino acids 1 to 54 were important for the interaction or conformational constraints imposed through residues 177 to 341 inhibited the interaction. In this study, deletion analysis of the RPM1 NB-ARC domain localized the RIN13/RPM1 binding interface within the region of RIN4 binding. Amino acids 28 to 54 were essential for RIN13 binding, indicating RIN13 occupies at least partially similar or overlapping RPM1 binding sites with RIN4, or these amino acids are essential to stabilize the tertiary NB-ARC structure necessary for both RIN4 and RIN13 binding. No interaction was detected between RIN13 and full-length RPM1 in yeast or in vitro, suggesting the conformation adopted by the LRR domain obscures the RIN13 binding site. Similar constraints appear to restrict RIN4 binding. Only a small percentage of RPM1 was coimmunoprecipitated with RIN4 in vivo, suggesting a transient association (Mackey et al., 2002) but also consistent with the promiscuous nature of RIN4's association with AvrRpt2 and RPS2 (Axtell and Staskawicz, 2003; Mackey et al., 2003). We are currently addressing the relationship of RIN4 with RIN13 and RPM1 in planta, but these studies are complicated by the low RIN13 expression and potential posttranslational modifications.

To reconcile our RIN13 data within the dual frameworks of the guard hypothesis and strict R protein conformational requirements, we propose a model (summarized in Figure 8) based upon the following considerations: (1) additional RIN proteins associated with RPM1 are themselves likely to be involved in other protein–protein interactions, (2) the molecular architecture of the signaling complex is predicted to be large and some interactions transient, and (3) a conformational change is necessary to expose the RIN13 binding site within the NB-ARC domain. We hypothesize that intramolecular conformational changes after RPM1 elicitation (AvrRpm1 delivery) expose the NB-ARC domain and facilitate binding of RIN13, where it collaborates to activate pathways leading to bacterial restriction. In the absence of RIN13, bacterial restriction signaling mechanisms are attenuated, but attendant signaling mechanisms specifying hypersensitive cell death are unaffected.

When overexpressed, *RIN13* abrogates hypersensitive cell death and enhances resistance after RPM1 elicitation. That ectopic expression of *RIN13* abolishes the HR but enhances resistance implies that excess of RIN13 restricts accessibility for signaling component(s) mediating hypersensitive cell death pathways or imposes local conformational limitations preventing additional cofactors necessary for transducing the HR signal from binding or being released. *RIN13s* overexpression did not modify the mutant phenotype in both *Atrar1* and *rpm1* backgrounds, indicating RIN13 function is dependent upon RPM1.

In conclusion, we report a protein that positively and very selectively modulates bacterial resistance responses. Our data support a specific and critical role for RIN13 in transduction of an effective RPM1 resistance response. As tools are developed to overcome sensitivity issues, comparisons of elicited complexes in *RIN13s/as* lines with the wild type should further illuminate the nature of the resistosome.

Minimal impact on trait qualities is a major consideration for crop improvement. *RIN13* lines show no morphological and developmental defects, such as those reported in transgenic lines engineered for reduced expression of the RPM1 interactors *RIN4* (Mackey et al., 2002) and *AtTIP49* (Holt et al., 2002). Moreover, leaves in *RIN13s/as* lines responded identically to pathogens delivering *avrRpm1*, whereas in *RIN4as* plants, a stochastic response to AvrRpm1 delivery was reported (only ~30% of challenged leaves were compromised for the HR; Mackey et al., 2002). Our results therefore suggest a real possibility of engineering-enhanced resistance in the absence of programmed cell death.

METHODS

Chemicals

All chemicals were from Sigma-Aldrich (Gillingham, Dorset, UK) unless specified.

Pseudomonas Maintenance and Pathogen Challenge

Pseudomonas syringae pv *tomato* DC3000 containing the appropriate avirulence gene cloned into the broad host range vector pVSP61 (Innes et al., 1993) or pVSP61 alone as a virulent control were maintained under selection, cultured, and used for pathogen challenge as described (Murillo and Keen, 1994; Grant et al., 1995). Final cell densities were adjusted to A_{600} 0.05 (2×10^7 cfu/mL) for HR phenotyping, ion leakage assays, DAB polymerization, biophoton emission studies, or trypan blue staining. For bacterial population studies, A_{600} 0.0002 (0.8×10^5 cfu/mL) was used. Challenged leaves of 5- to 6-week-old plants (three plants, four leaves/plant) were sampled 0, 2, and 4 d postinoculation. All bacterial growth experiments were repeated at least three times.

Growth of Plants

Arabidopsis thaliana lines for pathotesting were grown for 5 to 6 weeks under short days to encourage robust rosette formation (de Torres et al., 2003).

Yeast Methods

All yeast methods were as described (Bartel and Fields, 1997). Baits for the two-hybrid screen were subcloned from a full-length *RPM1* genomic clone (Grant et al., 1995) into pEG202 and were first verified for nuclear localization and absence of transcriptional activation of *LacZ* in pJK101. The pathogen-challenged Col-0 leaf library was constructed in pJG4-5 and has been previously described (Holt et al., 2002). All library screening and bait deletion analyses used the yeast strain EGY48. Library screens were initially selected for complementation of Leu auxotrophy on Gal/Raf ura^- his^- trp^- leu^- media, and subsequently putative interactors were tested for β-galactosidase activity on Gal/Raf ura^- his^- trp^- media containing X-gal. Plasmids containing the putative interactors were then isolated and reintroduced into the original yeast bait lines or a series of control bait lines to verify the efficacy of the interaction.

Constructs and Transgenic Lines

A full-length *RIN13* cDNA clone (*pBSRIN13*) was isolated using a partial clone derived from pJG4-5 screen and sequence verified. A *Nco*I site was inserted at the initiating ATG by oligonucleotide-mediated mutagenesis using the primer 5′-GTTACGAAAATTTTGTC**C**ATGGGTTCGGGTA-ATC-3′ (bold indicates the mutagenized nucleotide). The complete *RIN13* cDNA was then excised as an ~1200-bp *Nco*I and *Sma*I fragment and

ligated into *Nco*I/*Pml*I cut and dephosphorylated pCAMBIA3201 (www.cambia.org.au/), generating full-length *RIN13* under control of the strong viral 35S promoter of *Cauliflower mosaic virus*. For antisense lines, a 600-bp *RIN13 Ava*II/*Hin*dIII fragment was blunt-end ligated into polished *Bst*EII/*Bgl*II pCAMBIA3301. Both *RIN13s* and *RIN13as* binary constructs were introduced into *Agrobacterium tumefaciens* GV3101 (pMP90) and transformed into Col-5, *rpm1*-3, or *Atrar1*-28 by the floral dip method (Clough and Bent, 1998). Transgenic plants were selected using glufosinate ammonium (Hoescht, Frankfurt, Germany) at 150 mg/L.

The T-DNA insertion allele Δ*RIN13* was identified in the SIGnAL T-DNA Express library (Alonso et al., 2003). A line with a single insertion (see Supplemental Figure 1 online) was identified and carried to homozygosity. Δ*RIN13* was also introduced into Col-5 by selecting for homozygous Δ*RIN13* glabrous plants in the F2.

Generation of the DEX:*avrRpm1* line is described by Bennett et al. (2005).

Measuring HR Parameters

Ion Leakage

Immediately after infiltration, 12 leaf discs from three plants were removed with a cork borer (number 6) and floated adaxial side up in 50 mL of distilled water. After 15 min, the discs were transferred to 25 mL of fresh water and conductance measured.

Trypan Blue Staining

Plant cell death was monitored by trypan blue staining using lactophenol-trypan blue solution as previously described (Koch and Slusarenko, 1990). Stained tissue was cleared and subsequently stored in 2.5 g/mL (w/v) of chloral hydrate.

H_2O_2 Detection by DAB Polymerization

Pathogen-challenged leaves were harvested at various times after infiltration, immediately placed in 1 mg/mL of DAB-HCl, pH 3.8 (Thordal-Christensen et al., 1997), and incubated for 6 h in the dark at room temperature. Treated leaves were cleared in boiling ethanol.

Biophoton Imaging

Biophoton emissions were measured in pathogen-challenged plants as described by Bennett et al. (2005). Pathogen-challenged plants were placed inside a dark box, and bioluminescence was captured using a Hamamatsu ORCAII ER CCD camera (Hamamatsu City, Japan) fitted with a 35-mm f2.8 Nikon lens (Tokyo, Japan). Photons were counted for 15 min at 2 × 2 binning mode and images acquired using Wasabi imaging software (Hamamatsu).

RNA Gel Blot Analysis

A minimum of four leaves on six plants was mock- or pathogen-infiltrated and samples collected at the appropriate time and immediately frozen in liquid N_2. RNA isolation and RNA gel blots were as described (de Torres et al., 2003). RNA loading was determined by hybridization to *A. thaliana Actin 2* (At3g18780). All RNA gel blots are representative of at least two independent experiments.

In Vitro Pull-Down Experiments

Preparation of RPM1 Expressing Yeast Extracts

HA epitope–tagged RPM1 fragments F1 and F2 were generated by subcloning the baits (Figure 1) from pEG202 into the prey vector pJG4-5 and inducing in yeast strain EGY48 containing the reporter plasmid pSH18-34 and control plasmid pRFHM1. Overnight yeast cultures (10 mL *ura*$^-$*his*$^-$*trp*$^-$ synthetic complete media containing 2% glucose) were used to inoculate fresh 250-mL cultures containing either 2% glucose (off) or 2% galactose/1% raffinose (on). Cells were harvested by centrifugation after incubation at 28°C overnight. Cell pellets were resuspended to 2.5 mL in yeast lysis buffer (50 mM Tris-HCl, pH 8, 200 mM NaCl, 1 mM EDTA, 1 mM PMSF, and 1 μg/mL leupeptin) and vortexed for 5 min with 500 μL of acid-washed glass beads (Sigma-Aldrich G-1277). Crude extracts were clarified by centrifugation and aliquots prepared to avoid freeze-thaw cycles.

Preparation of RIN13 Extracts

RIN13 was cloned into the pTWIN1 vector (New England Biolabs, Beverly, MA) as a *Nco*I-*Xho*I fragment and expressed in Codon$^+$ cells (Stratagene, La Jolla, CA) to create an in-frame fusion with the *Synechocytis* sp DnaB intein (Intein-RIN13). As a control, induction of the empty pTWIN1 vector generated a chimeric fusion between the *Synechocytis* sp DnaB and *Mycobacterium xenopi* Gyrase A Inteins (intein). Crude bacterial extracts expressing intein-RIN13 or intein were harvested by centrifugation and resuspended in 40 mL of Buffer B (20 mM Tris-HCl, pH 8.5, 500 mM NaCl, and 1 mM EDTA). Extracts were normalized for intein expression.

Immunoprecipitation of RPM1

Equal amounts of target intein (~800 μg of total Intein-RIN13 or 200 μg of intein crude bacterial extracts) were made up to 500 μL in Buffer B and added to 30 μL of chitin beads (NEB) prewashed in buffer B. These mixtures were incubated for 1.5 h at 4°C with shaking, then washed four times in Buffer B and twice in immunoprecipitation (IP) buffer (50 mM NaCl, 50 mM Tris-HCl, pH 8.0, 10 mM EDTA, and 0.2% Triton X-100). To pull down F1- or F2-RPM1, 500 μL of IP buffer and 50 μL of yeast extracts containing 35 and 30 μg, respectively, of crude protein were added to chitin beads containing the bound RIN13-Intein or intein and incubated for 2 h at 4°C with shaking. The beads were then washed in IP buffer (1 mL) for 5 min with shaking, four times at 4°C. Finally, 40 μL of 2× SDS-PAGE buffer was added to the final washed beads, and samples were run on 12% SDS-PAGE, blotted to PDF membrane (Amersham, Buckinghamshire, UK), and visualized with anti-HA antibody (Roche, Indianapolis, IN) by ECL (Amersham).

ACKNOWLEDGMENTS

We thank Wendy Byrne for excellent technical assistant and John Mansfield for helpful discussions and critical reading of the manuscript. We thank the Nottingham Arabidopsis Stock Centre for supplying the Salk insertion seed. This research was supported by the Biotechnology and Biological Science Research Council (Grants ICR07542 and P18600).

Received October 21, 2004; accepted December 20, 2004.

REFERENCES

Adams, J.M., and Cory, S. (2002). Apoptosomes: Engines for caspase activation. Curr. Opin. Cell Biol. **14,** 715–720.

Alonso, J.M., et al. (2003). Genome-wide insertional mutagenesis of *Arabidopsis thaliana*. Science **301,** 653–657.

Aravind, L., Dixit, V.M., and Koonin, E.V. (1999). The domains of death: Evolution of the apoptosis machinery. Trends Biochem. Sci. **24,** 47–53.

Axtell, M.J., and Staskawicz, B.J. (2003). Initiation of RPS2-specified disease resistance in Arabidopsis is coupled to the AvrRpt2-directed elimination of RIN4. Cell **112,** 369–377.

Balague, C., Lin, B., Alcon, C., Flottes, G., Malmstrom, S., Kohler, C., Neuhaus, G., Pelletier, G., Gaymard, F., and Roby, D. (2003). HLM1, an essential signaling component in the hypersensitive response, is a member of the cyclic nucleotide-gated channel ion channel family. Plant Cell **15,** 365–379.

Banerjee, D., Zhang, X., and Bent, A.F. (2001). The leucine-rich repeat domain can determine effective interaction between RPS2 and other host factors in arabidopsis RPS2-mediated disease resistance. Genetics **158,** 439–450.

Bartel, P.L., and Fields, S. (1997). The Yeast Two-Hybrid System. (New York: Oxford University Press).

Bennett, M., Mehta, M., and Grant, M. (2005). Biophoton imaging: A nondestructive method for assaying *R* gene responses. Mol. Plant-Microbe Interact. **18,** 95–102.

Bestwick, C.S., Brown, I.R., and Mansfield, J.W. (1998). Localized changes in peroxidase activity accompany hydrogen peroxide generation during the development of a nonhost hypersensitive reaction in lettuce. Plant Physiol. **118,** 1067–1078.

Bonas, U., and Lahaye, T. (2002). Plant disease resistance triggered by pathogen-derived molecules: Refined models of specific recognition. Curr. Opin. Microbiol. **5,** 44–50.

Boyes, D.C., Nam, J., and Dangl, J.L. (1998). The *Arabidopsis thaliana* RPM1 disease resistance gene product is a peripheral plasma membrane protein that is degraded coincident with the hypersensitive response. Proc. Natl. Acad. Sci. USA **95,** 15849–15854.

Buttner, D., and Bonas, U. (2003). Common infection strategies of plant and animal pathogenic bacteria. Curr. Opin. Plant Biol. **6,** 312–319.

Century, K.S., Holub, E.B., and Staskawicz, B.J. (1995). NDR1, a locus of *Arabidopsis thaliana* that is required for disease resistance to both a bacterial and a fungal pathogen. Proc. Natl. Acad. Sci. USA **92,** 6597–6601.

Century, K.S., Shapiro, A.D., Repetti, P.P., Dahlbeck, D., Holub, E., and Staskawicz, B.J. (1997). NDR1, a pathogen-induced component required for Arabidopsis disease resistance. Science **278,** 1963–1965.

Clough, S.J., and Bent, A.F. (1998). Floral dip: A simplified method for Agrobacterium-mediated transformation of *Arabidopsis thaliana*. Plant J. **16,** 735–743.

Clough, S.J., Fengler, K.A., Yu, I.C., Lippok, B., Smith, R.K., Jr., and Bent, A.F. (2000). The Arabidopsis dnd1 ''defense, no death'' gene encodes a mutated cyclic nucleotide-gated ion channel. Proc. Natl. Acad. Sci. USA **97,** 9323–9328.

Dangl, J.L., and Jones, J.D. (2001). Plant pathogens and integrated defence responses to infection. Nature **411,** 826–833.

Deslandes, L., Olivier, J., Peeters, N., Feng, D.X., Khounlotham, M., Boucher, C., Somssich, I., Genin, S., and Marco, Y. (2003). Physical interaction between RRS1-R, a protein conferring resistance to bacterial wilt, and PopP2, a type III effector targeted to the plant nucleus. Proc. Natl. Acad. Sci. USA **100,** 8024–8029.

de Torres, M., Sanchez, P., Fernandez-Delmond, I., and Grant, M. (2003). Expression profiling of the host response to bacterial infection: The transition from basal to induced defence responses in RPM1-mediated resistance. Plant J. **33,** 665–676.

Eckardt, N.A., and Innes, R. (2003). Resistance rodeo: Rounding up the full complement of Arabidopsis NBS-LRR genes. Plant Cell **15,** 806–807.

Espinosa, A., Guo, M., Tam, V.C., Fu, Z.Q., and Alfano, J.R. (2003). The *Pseudomonas syringae* type III-secreted protein HopPtoD2 possesses protein tyrosine phosphatase activity and suppresses programmed cell death in plants. Mol. Microbiol. **49,** 377–387.

Flor, H.H. (1971). Current status of the gene-for-gene concept. Annu. Rev. Phytopathol. **9,** 275–296.

Grant, J.J., and Loake, G.J. (2000). Role of reactive oxygen intermediates and cognate redox signaling in disease resistance. Plant Physiol. **124,** 21–29.

Grant, M., Brown, I., Adams, S., Knight, M., Ainslie, A., and Mansfield, J. (2000). The RPM1 plant disease resistance gene facilitates a rapid and sustained increase in cytosolic calcium that is necessary for the oxidative burst and hypersensitive cell death. Plant J. **23,** 441–450.

Grant, M., and Mansfield, J. (1999). Early events in host-pathogen interactions. Curr. Opin. Plant Biol. **2,** 312–319.

Grant, M.R., Godiard, L., Straube, E., Ashfield, T., Lewald, J., Sattler, A., Innes, R.W., and Dangl, J.L. (1995). Structure of the Arabidopsis RPM1 gene enabling dual specificity disease resistance. Science **269,** 843–846.

Grant, M.R., McDowell, J.M., Sharpe, A.G., de Torres Zabala, M., Lydiate, D.J., and Dangl, J.L. (1998). Independent deletions of a pathogen-resistance gene in Brassica and Arabidopsis. Proc. Natl. Acad. Sci. USA **95,** 15843–15848.

Hammond-Kosack, K.E., and Parker, J.E. (2003). Deciphering plant-pathogen communication: Fresh perspectives for molecular resistance breeding. Curr. Opin. Biotechnol. **14,** 177–193.

Holt III, B.F., Boyes, D.C., Ellerstrom, M., Siefers, N., Wiig, A., Kauffman, S., Grant, M.R., and Dangl, J.L. (2002). An evolutionarily conserved mediator of plant disease resistance gene function is required for normal Arabidopsis development. Dev. Cell **2,** 807–817.

Holub, E.B., Brose, E., Tor, M., Clay, C., Crute, I.R., and Beynon, J.L. (1995). Phenotypic and genotypic variation in the interaction between *Arabidopsis thaliana* and *Albugo candida*. Mol. Plant Microbe Interact. **8,** 916–928.

Innes, R.W., Bent, A.F., Kunkel, B.N., Bisgrove, S.R., and Staskawicz, B.J. (1993). Molecular analysis of avirulence gene avrRpt2 and identification of a putative regulatory sequence common to all known *Pseudomonas syringae* avirulence genes. J. Bacteriol. **175,** 4859–4869.

Inohara, N., and Nunez, G. (2001). The NOD: A signaling module that regulates apoptosis and host defense against pathogens. Oncogene **20,** 6473–6481.

Inohara, N., and Nunez, G. (2003). NODs: Intracellular proteins involved in inflammation and apoptosis. Nat. Rev. Immunol. **3,** 371–382.

Jia, Y., McAdams, S.A., Bryan, G.T., Hershey, H.P., and Valent, B. (2000). Direct interaction of resistance gene and avirulence gene products confers rice blast resistance. EMBO J. **19,** 4004–4014.

Jin, Q., Thilmony, R., Zwiesler-Vollick, J., and He, S.Y. (2003). Type III protein secretion in *Pseudomonas syringae*. Microbes Infect. **5,** 301–310.

Jones, D.A., and Jones, J.D.G. (1996). The role of leucine-rich repeat proteins in plant defences. Adv. Bot. Res. **24,** 91–167.

Klement, Z. (1982). Hypersensitivity. (New York: Academic Press).

Kobe, B., and Kajava, A.V. (2001). The leucine-rich repeat as a protein recognition motif. Curr. Opin. Struct. Biol. **11,** 725–732.

Koch, E., and Slusarenko, A. (1990). Arabidopsis is susceptible to infection by a downy mildew fungus. Plant Cell **2,** 437–445.

Liu, Y., Burch-Smith, T., Schiff, M., Feng, S., and Dinesh-Kumar, S.P. (2004). Molecular chaperone Hsp90 associates with resistance protein N and its signaling proteins SGT1 and Rar1 to modulate an innate immune response in plants. J. Biol. Chem. **279,** 2101–2108.

Luck, J.E., Lawrence, G.J., Dodds, P.N., Shepherd, K.W., and Ellis, J.G. (2000). Regions outside of the leucine-rich repeats of flax rust resistance proteins play a role in specificity determination. Plant Cell **12,** 1367–1377.

Mackey, D., Belkhadir, Y., Alonso, J.M., Ecker, J.R., and Dangl, J.L. (2003). Arabidopsis RIN4 is a target of the type III virulence effector AvrRpt2 and modulates RPS2-mediated resistance. Cell **112,** 379–389.

Mackey, D., Holt, B.F., Wiig, A., and Dangl, J.L. (2002). RIN4 interacts with *Pseudomonas syringae* type III effector molecules and is required for RPM1-mediated resistance in Arabidopsis. Cell **108,** 743–754.

Martin, G.B., Bogdanove, A.J., and Sessa, G. (2003). Understanding the functions of plant disease resistance proteins. Annu. Rev. Plant Biol. **54,** 23–61.

Meyers, B.C., Kozik, A., Griego, A., Kuang, H., and Michelmore, R.W. (2003). Genome-wide analysis of NBS-LRR-encoding genes in Arabidopsis. Plant Cell **15,** 809–834.

Moffett, P., Farnham, G., Peart, J., and Baulcombe, D.C. (2002). Interaction between domains of a plant NBS-LRR protein in disease resistance-related cell death. EMBO J. **21,** 4511–4519.

Murillo, J., and Keen, N.T. (1994). Two native plasmids of *Pseudomonas syringae* pathovar tomato strain PT23 share a large amount of repeated DNA, including replication sequences. Mol. Microbiol. **12,** 941–950.

Muskett, P.R., Kahn, K., Austin, M.J., Moisan, L.J., Sadanandom, A., Shirasu, K., Jones, J.D., and Parker, J.E. (2002). Arabidopsis RAR1 exerts rate-limiting control of R gene-mediated defenses against multiple pathogens. Plant Cell **14,** 979–992.

Schulze-Lefert, P. (2004). Plant immunity: The origami of receptor activation. Curr. Biol. **14,** R22–R24.

Shao, F., Golstein, C., Ade, J., Stoutemyer, M., Dixon, J.E., and Innes, R.W. (2003). Cleavage of Arabidopsis PBS1 by a bacterial type III effector. Science **301,** 1230–1233.

Shirasu, K., Lahaye, T., Tan, M.W., Zhou, F., Azevedo, C., and Schulze-Lefert, P. (1999). A novel class of eukaryotic zinc-binding proteins is required for disease resistance signaling in barley and development in *C. elegans*. Cell **99,** 355–366.

Shirasu, K., and Schulze-Lefert, P. (2003). Complex formation, promiscuity and multi-functionality: Protein interactions in disease-resistance pathways. Trends Plant Sci. **8,** 252–258.

Swiderski, M.R., and Innes, R.W. (2001). The Arabidopsis PBS1 resistance gene encodes a member of a novel protein kinase subfamily. Plant J. **26,** 101–112.

Tameling, W.I., Elzinga, S.D., Darmin, P.S., Vossen, J.H., Takken, F.L., Haring, M.A., and Cornelissen, B.J. (2002). The tomato R gene products I-2 and MI-1 are functional ATP binding proteins with ATPase activity. Plant Cell **14,** 2929–2939.

Tao, Y., Xie, Z., Chen, W., Glazebrook, J., Chang, H.S., Han, B., Zhu, T., Zou, G., and Katagiri, F. (2003). Quantitative nature of Arabidopsis responses during compatible and incompatible interactions with the bacterial pathogen *Pseudomonas syringae*. Plant Cell **15,** 317–330.

Thordal-Christensen, H., Zhang, Z., Wei, Y., and Collinge, D.B. (1997). Subcellular localisation of H_2O_2 in plants. H_2O_2 accumulation in papillae and hypersensitive response during the barley-powdery mildew interaction. Plant J. **11,** 1187–1194.

Tornero, P., Chao, R.A., Luthin, W.N., Goff, S.A., and Dangl, J.L. (2002a). Large-scale structure-function analysis of the Arabidopsis RPM1 disease resistance protein. Plant Cell **14,** 435–450.

Tornero, P., Merritt, P., Sadanandom, A., Shirasu, K., Innes, R.W., and Dangl, J.L. (2002b). RAR1 and NDR1 contribute quantitatively to disease resistance in Arabidopsis, and their relative contributions are dependent on the R gene assayed. Plant Cell **14,** 1005–1015.

Torres, M.A., Dangl, J.L., and Jones, J.D. (2002). Arabidopsis gp91phox homologues AtrbohD and AtrbohF are required for accumulation of reactive oxygen intermediates in the plant defense response. Proc. Natl. Acad. Sci. USA **99,** 517–522.

Tschopp, J., Martinon, F., and Burns, K. (2003). NALPs: A novel protein family involved in inflammation. Nat. Rev. Mol. Cell Biol. **4,** 95–104.

Van der Biezen, E.A., and Jones, J.D. (1998). Plant disease-resistance proteins and the gene-for-gene concept. Trends Biochem. Sci. **23,** 454–456.

van der Biezen, E.A., and Jones, J.D. (1998). The NB-ARC domain: A novel signalling motif shared by plant resistance gene products and regulators of cell death in animals. Curr. Biol. **8,** R226–R227.

van der Biezen, E.A., Sun, J., Coleman, M.J., Bibb, M.J., and Jones, J.D. (2000). Arabidopsis RelA/SpoT homologs implicate (p)ppGpp in plant signaling. Proc. Natl. Acad. Sci. USA **97,** 3747–3752.